[Article ID] 1003- 6326(2001)06- 0895- 05

Effect of constraint on crack propagation behavior in BGA soldered joints①

WANG Li(王 莉)[1], WANG Guo-zhong(王国忠)[1], FANG Hong-yuan(方洪渊)[2], QIAN Yi-yu(钱乙余)[2]
(1. DiamlerChrysler SIM Technology Co, Ltd, Chinese Academy of Science, Shanghai 200050, P. R. China;
2. National Key laboratory of Advanced Welding Production Technology, Harbin Institute of Technology, Harbin 150001, P. R. China)

[Abstract] The effects of stress triaxiality on crack propagation behavior in the BGA soldered joint were analyzed using FEM method. The computation results verified that stress triaxiality factor has an important effect on crack growth behavior. Crack growth rate increased with increasing stress triaxiality at the near-tip region, which is caused by increasing crack lengths or decreasing solder joint heights. Solder joint deformation is subjected to constraint effect provided by its surrounding rigid ceramic substrate, the constraint can be scaled by stress triaxiality near crack tip region. Therefore, it can be concluded that crack growth rate increased when the constraint effect increases.

[Key words] constraint; crack; behavior; joints
[CLC number] TG 404 [Document code] A

1 INTRODUCTION

The reliability of solder joints is one of the critical issues in Surface Mount Technology (SMT) field[1~3]. The more severe service environmental conditions of electronic devices in automotive application, and the development of advanced interconnection technologies for area array packages demand higher solder joint reliability, which have focused on the investigation of solder joint failure[4~7].

A number of previous researchers have proposed that solder joints failure was caused by creep and fatigue damages during thermal cycling, the main mechanism is thermal stress and low cycle strain-controlled fatigue[8,9]. Therefore, Coffin-Manson equation was widely used to predict the fatigue life of solder joints[10~12]. In the equation, the accumulated inelastic strain (creep strain and plastic strain) was assumed to be the mechanical factor that governed the failure of solder joints. In fact, the deformation and the fracture behavior of solder joints were different from that of bulk solder alloys. The typical PBGA solder joints were usually formed with SnPb eutectic alloy as interlayer attached by Si chip and FR4 board. From the viewpoint of mechanics, the solder joints were equivalent to low strength match mechanical heterogeneity. In other words, the plastic deformations of BGA solder joints were constrained by its surrounding stiffer material. In addition, under thermal cycling loading conditions, solder joints were in a state of complicated stresses that are composed of tension stress and shear stress. Therefore, it can be expected that the constraint effect will play an important part in high temperature deformation and rupture behavior of soldered joints. But unfortunately, all of previous research works neglect the effect of constraint on solder joint reliability.

In the present paper, the ADINA finite element analysis program[13] was used to analyze stress-strain fields near the crack tip region in the BGA solder joints. The emphasis was put on the effect of the constraint on crack growth behavior of BGA solder joints.

2 FEM MODEL DEVELOPMENT

The simulated BGA sample was used to analyze the effect of constraint on the stress-strain field near the crack tip in the BGA solder joints. In the realistic PBGA packages, silicon chip was attached to PCB board with Sn-Pb eutectic solder balls. The most critical solder joints are the ones closest to the edge of silicon chip because there is the most serious CTE (coefficient of thermal expansion) mismatch between silicon chip and PCB board[11]. In the simulated BGA samples, alumina ceramic chip was used to simulate the realistic BGA packages since there was larger CTE mismatch between alumina ceramic substrate and PCB board, which is accordant to realistic BGA package. The specimen geometry was shown in Fig. 1. It has a alumina ceramic substrate connected to an FR4 board with four Sn-Pb eutectic solder joints at each end. A molybdenum pad with 1.0 mm pad diameter is used as the ceramic connection and the cop-

① [Foundation item] Project 1805 supported by 211 project Fund of Harbin Institute of Technology
[Received date] 2001- 02- 19; [Accepted date] 2001- 06- 11

per pad with 0.8 mm pad diameter is for the FR4 connection. The analysis used a 2-dimensional plane strain model. The representative mesh is shown in Fig. 2, which corresponds to the cross section of the specimen in y-z plane. All parts of the model consist of 4-node plane strain elements. Due to symmetry, only half of the BGA sample was modeled. In this model, the boundary conditions can be described as follows:

$$\left.\begin{aligned} u_y &= 0,\ y = 0 \\ u_z &= 0,\ y = z = 0 \end{aligned}\right\} \quad (1)$$

where u_y, u_z are the displacement along y and z axises, respectively.

In this model, temperature-independent linear elastic material models were assumed for Al_2O_3 ceramic chip and FR4 board. The corresponding material constants were summarized in Table 1. The constants are from Ref. [14].

Table 1 Material properties for Al_2O_3 ceramic chip and FR4 board[14]

Material	E / MPa	υ	CTE (10^{-6}/ ℃)
Al_2O_3 ceramic	3.79×10^5	0.21	5.3
FR4 board	1.11×10^4	0.28	20

A viscoplastic constitutive model was assumed for the 63Sn/37Pb solder to account for its time-dependent inelastic behavior during thermal cycling. Temperature-dependent elastic-plastic material prop-

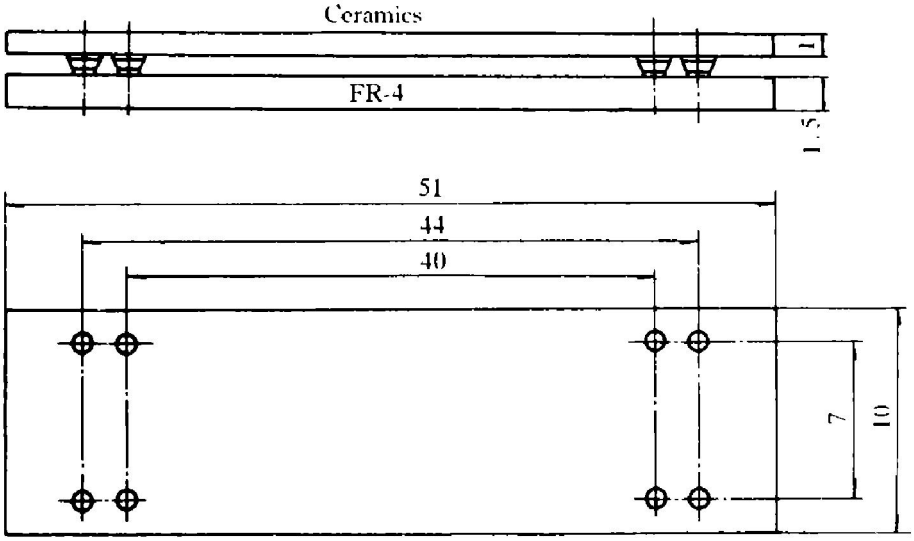

Fig. 1 Schematic of BGA simulated sample

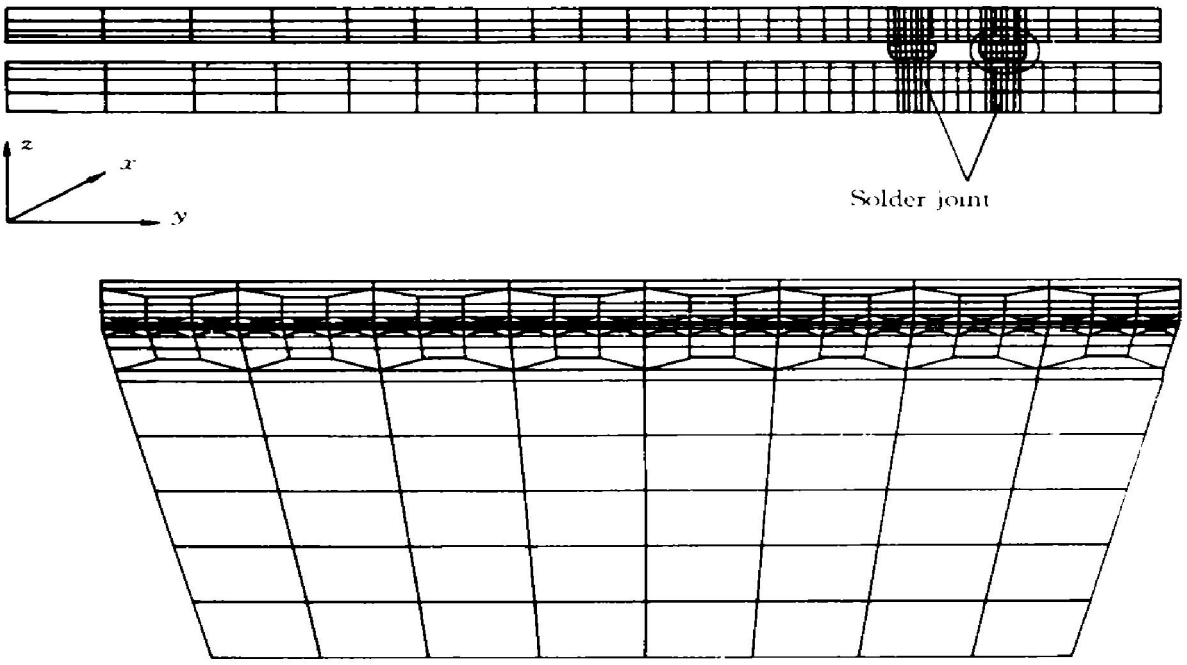

Fig. 2 2-dimensional FEM model of BGA sample

erties were listed in Table 2, they are obtained from Ref. [15].

Table 2 Elastic-plastic material properties for 63Sn/37Pb solder alloy[15]

Material property	Temperature/ ℃	
	− 55	125
Elastic modulus/ MPa	17.958	12.738
Possion's ratio	0.353	0.383
CTE(10^{-6}/ ℃)	21.0	21.0
Yield stress/ MPa	48.23	8.05
Tangent modulus/ MPa	897.9	636.9

The steady creep behavior was assumed to follow Weertman's rule[16]

$$\dot{\varepsilon}_c = \varepsilon_0 \cdot \bar{\sigma}^{n_c} \cdot e^{-\frac{\Delta H}{kT}} \tag{3}$$

where $\dot{\bar{\varepsilon}}$ is equivalent creep strain rate, s^{-1}; σ is the effective stress, MPa; n_c is the stress exponent, $n_c = 0.159$; ΔH is the activation energy, $\Delta H = 1.13 \times 10^{-19}$ (J/ mol); T is the absolute temperature, K; k is the Boltzmann's constant, $k = 1.38 \times 10^{-23}$ (J/ K); ε_0 is material constant, $\varepsilon_0 = 6.286 \times 10^{-15}$.

In FEM analysis, The loading is 10 s ramp and 30 min hold time thermal cycling between − 55 ℃ and 125 ℃. The highest temperature 125 ℃ is treated as the initially stress-free temperature.

Since highest stress concentrated at the interface between ceramic substrate and solder alloy in the outside solder joints, the initial crack was defined at the interface. Initially it was assumed that the crack was 0.125 mm long, then grew up to 0.625 mm. Finite element analysis was carried out for six different crack lengths. In order to prevent the embedment between crack surfaces, the crack surfaces were defined as contact surfaces. In order to vary the constraint provided by the rigid ceramic substrate, on one hand, six different crack lengths were chosen, they were 0.125, 0.250, 0.333, 0.416, 0.500 and 0.625 mm, respectively. On the other hand, two solder joint heights were used, one was 0.450 mm, the other was 0.375 mm.

3 RESULTS AND DISCUSSION

In the paper, hydrostatic stress was expressed as σ_h by

$$\sigma_h = (\sigma_1 + \sigma_2 + \sigma_3)/3$$

where σ_1, σ_2, σ_3 are the principal stress.

Stress triaxiality is expressed by $\sigma_h/\bar{\sigma}$, where $\bar{\sigma}$ is the Mises effective stress.

The near-tip stress field for an interface crack between ceramic substrate and solder alloy was described by fracture mechanics parameter, strain energy release rate G. Fig. 3 shows the variation of strain energy release rate range ΔG with crack length for different solder joint heights. It could be seen that ΔG increased with increasing crack length or decreasing solder joint height. Fig. 4 shows the variation of crack growth rate with crack length for different solder joint heights. From Fig. 4 it can be seen that crack growth rate increased with increasing crack lengths, or decreasing solder joint heights. It has the same changing trend with ΔG.

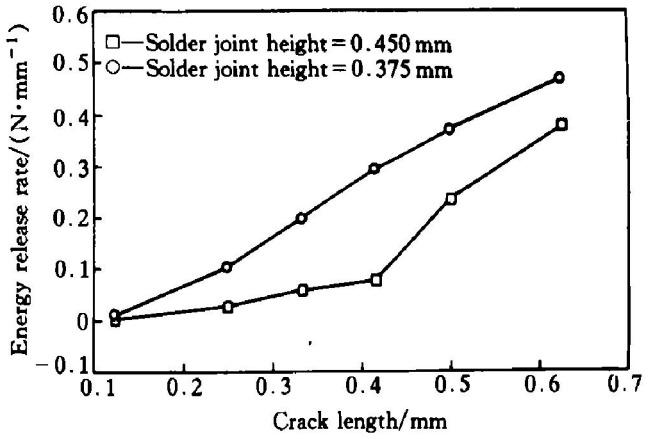

Fig. 3 Variation of strain energy release rate range with crack length for different solder joint heights

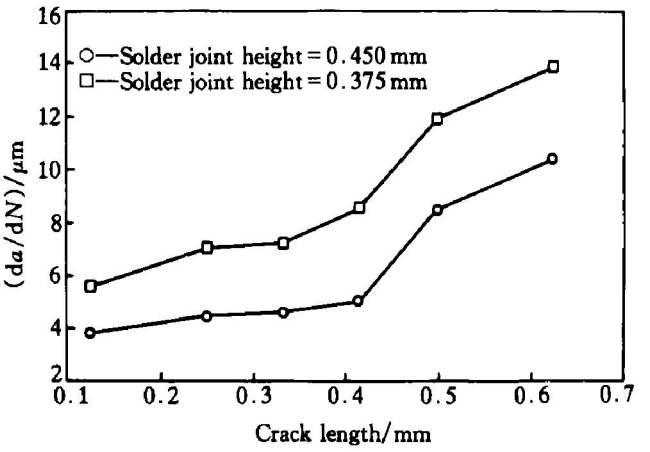

Fig. 4 Variation of crack growth rate with crack length for different solder joint heights

Stress-strain field near crack tip region for an interface crack between ceramic substrate and solder alloy determines crack propagation behavior in the solder joints. As mentioned above, solder joint is of low strength match mechanical heterogeneity, in which higher hydrostatic stress produced. Fig. 5 and Fig. 6 were the corresponding stress triaxiality and creep strain distribution at the front of crack tip under different crack lengths, respectively. From Fig. 5 and Fig. 6 we can see that stress triaxiality and equivalent creep strain increased with increasing crack length. Distribution of stress triaxiality at the front of crack tip reflects the changing trend of solder joint deformation constraint provided by its surrounding material.

From the point of view of energy balance, stress triaxilality increased at the crack tip with crack length, that indicated that elastic energy stored in cracking body increases, crack propagation driving force increases, i. e. energy release rate increases. Correspondingly, crack growth rate increases with increasing crack length, as shown in Fig. 3 and Fig. 4. Equivalent creep strain increased with increasing crack lengths, which indicated that energy dissipated increases in the process of crack growth, crack growth resistance increases. That also illustrated that crack growth is in a phase of steady propagation, and most of the elastic energy released in the process of crack propagation is dissipated to form the plastic zone at the crack tip.

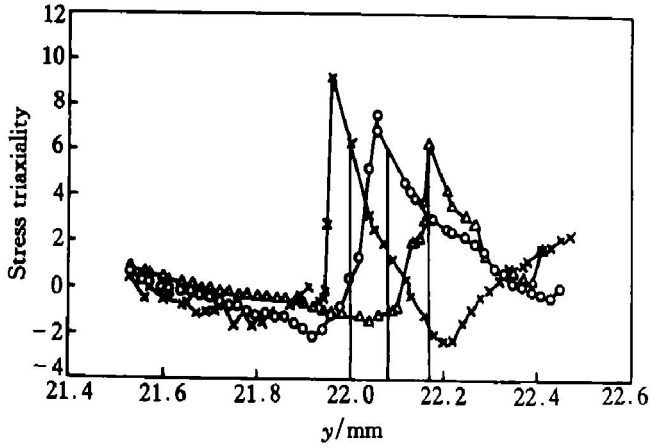

Fig. 5 Distribution of stress triaxiality at front of crack tip for different crack lengths

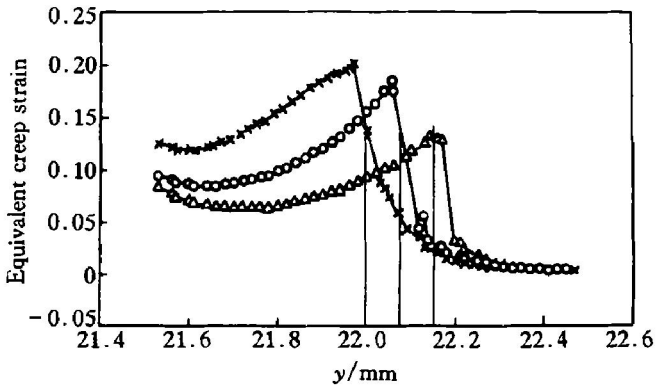

Fig. 6 Distribution of equivalent creep strain at front of crack tip for different crack lengths

Fig. 7 and Fig. 8 give the stress triaxiality and equivalent creep strain distribution near the crack tip under different solder joint heights. From Fig. 7 and Fig. 8 it can be seen that the stress triaxiality increased with decreasing solder joint height. That indicated that the solder joint deformation constraint effect provided by its surrounding material increases with reducing solder joint height. Similar to the above results, strain energy release rate range ΔG and crack growth rate increase with decreasing solder joint height, as shown in Fig. 3 and Fig. 4.

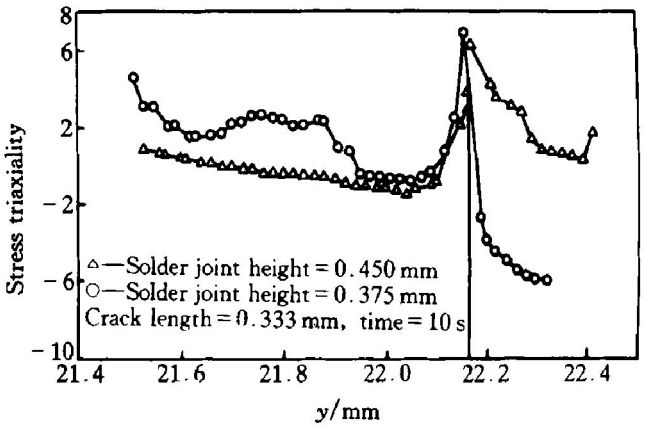

Fig. 7 Distribution of stress triaxiality at front of crack tip for different solder joint heights

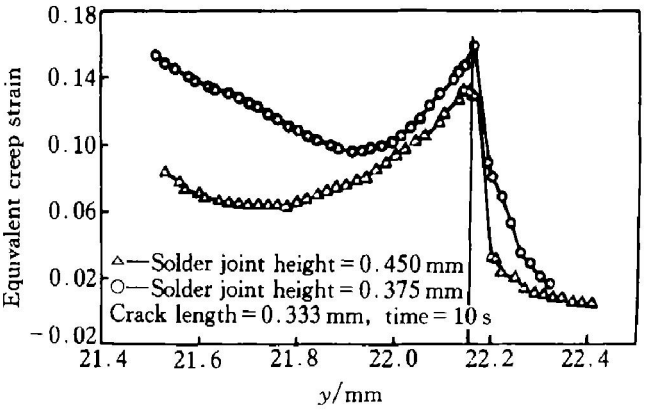

Fig. 8 Distribution of equivalent creep strain at front of crack tip for different solder joint heights

4 CONCLUSION

The solder joint deformation is subjected to constraint effect by the rigid ceramic substrate. The constraint can be scaled by stress triaxiality near crack tip region. FEM calculation results show that the constraint effect increases with increasing crack lengths or decreasing solder joint height. Crack growth rate increases correspondingly with increasing the constraint, which results in lower fatigue life of solder joint. Thus it seems that the constraint effect should be reduced in order to improve the reliability of solder joint.

[REFERENCES]

[1] Lau J H. Solder Joint Reliability: Theory and Applications, 1st Edition [M]. New York: Van Nostrand Reinhold, 1991.

[2] Lau J H, Pao Y H. Solder Joint Reliability of BGA, CSP, Flip Chip, and Fine Pitch SMT Assemblies, 1st Edition [M]. New York: McGraw-Hill, 1997.

[3] Lau J H. Thermal fatigue life prediction of flip chip solder joints by fracture mechanics method [J]. Internation-

al Journal of Engineering Fracture Mechanics, 1993, 45: 643- 654.

[4] Lau J H. Ball Grid Array Technology, 1st Edition [M]. New York: McGraw-Hill, Inc, 1995.

[5] Ries M D, Banks D R, Watson D P, et al. Attachment of solder ball connect packages to circuit cards [J]. IBM Journal of Research and Development, 1993, 37: 597- 607.

[6] Guo Y, Lim C K, Chen W T, et al. Solder ball connect assemblies under thermal loading Ⅰ—deformation measurement via more interferometry, and its interpretation [J]. IBM Journal of Research and Development, 1993, 37: 635- 647.

[7] Choi H C, Guo Y, Lafontaine W, et al. Solder ball connect assemblies under thermal loading Ⅱ—strain analysis via image processing and reliability considerations [J]. IBM Journal of Research and Development, 1993, 37: 649- 659.

[8] Liu D R, Yi-Hsin Pao. Fatigue-creep crack propagation path in solder joints under thermal cycling [J]. Journal of Electronic Materials, 1997, 26: 1060- 1064.

[9] Pao Yi-Hsin. A fracture mechanics approach to thermal fatigue life prediction of solder joints [J]. IEEE Trans CHMT, 1992, 15: 559- 570.

[10] Wong T E, Kachatorian L A, Tierney B D. Gull-wing solder joint fatigue life sensitivity evaluation [J]. Journal of Electronic Packaging, 1997, 119: 171- 176.

[11] Jung W, Lau J H, Pao Y H. Nonlinear analysis of full-matrix and perimeter plastic ball grid array solder joints [J]. Journal of Electronic Packaging, 1997, 119: 163 - 170.

[12] ZEN H B. Finite element modeling of thermal fatigue and damage of solder joints in a ceramic ball grid array package [J]. Journal of Electronic Materials, 1997, 26: 814- 820.

[13] Bath K J. ADINA/ADINAT/ADINAPLOT User Manual—Automatic Incremental Nonlinear Finite Element Program, 1st Edition [M]. Beijing: Mechanical Industry Press, 1986.

[14] Payder N, Botsis J. A finite element study of factors affecting fatigue life of solder joints [J]. Journal of Electronic Materials, 1994, 116: 265- 273.

[15] Busso E P, Kitano M, Kumazawa. A visocoplastic constitutive model for 60/40 tin-lead solder used in IC package joints [J]. ASME Journal of Engng Mat Tech, 1992, 114(7): 231- 237.

[16] Lau J H. Solder joint reliability of a low cost chip size package—NuCSP [J]. Microelectronics Reliability, 1998, 38: 1519- 1529.

(Edited by HUANG Jin-song)